JOURNAL OF ENERGY, MATERIALS, AND INSTRUMENTATION TECHNOLOGY

Journal Webpage https://jemit.fmipa.unila.ac.id/

Synthesis of ZnO/Ag Nanocomposites with Variatons of Zinc Nitrate Hexahydrate as an Antibacterial Agent against *Escherichia coli*

Zeiffa Alifia Maulita[a], Posman Manurung[b], Suprihatin, and Dwi Asmi

Department of Physics, Faculty of Mathematics and Natural Sciences, University of Lampung, Bandar Lampung, Indonesia, 35141

Article Information

Article history:
Received September 3, 2025
Received in revised form October 3, 2025
Accepted October 16, 2025

Keywords: *Antibacterial, Escherichia coli, Nanocomposites, Silver, Zinc Oxide*

Abstract

The synthesis of ZnO/Ag nanocomposites was carried out using different concentrations of $Zn(NO_3)_2.6H_2O$ precursors (0.04 M, 0.06 M, 0.08 M, and 0.1 M) by wet chemical precipitation. This study aimed to characterize the structure, morphology, and antibacterial activity of ZnO/Ag nanocomposites against Escherichia coli (E.coli). The characterization techniques used were X-Ray Fluorescence (XRF), X-Ray Diffraction (XRD), and Scanning Electron Microscopy with Energy Dispersive X-Ray (SEM-EDX). XRF analysis confirmed the presence of Zn as the main element and Ag as a dopant. XRD results showed that the ZnO/Ag nanocomposites exhibited a hexagonal wurtzite structure for ZnO and a Face-Centered Cubic (FCC) structure for Ag. SEM-EDX analysis revealed homogeneously distributed particles with nano-scale morphology. Antibacterial activity was tested using the disk diffusion method. The results indicated that the inhibition zone increased with higher $Zn(NO_3)_2.6H_2O$ concentration, proving that ZnO/Ag nanocomposites exhibit significant antibacterial properties against E.coli.

Informasi Artikel

Proses artikel:
Diterima 3 September 2025
Diterima dan direvisi dari 3 Oktober 2025
Accepted 16 Oktober 2025

Kata kunci: *Antibakteri, Escherichia coli, Nanokomposit, Perak, Seng Oksida*

Abstrak

Telah dilakukan sintesis nanokomposit ZnO/Ag menggunakan variasi konsentrasi precursor $Zn(NO_3)_2.6H_2O$ (0,04 M, 0,06 M, 0,08 M, dan 0,1 M) dengan metode presipitasi basah. Penelitian ini bertujuan untuk mengkarakterisasi struktur, morfologi, dan aktivitas antibakteri nanokomposit ZnO/Ag terhadap *Escherichia coli*. Karakterisasi dilakukan menggunakan *X-Ray Flourescence* (XRF), *X-Ray Diffraction* (XRD), dan *Scanning Electron Microscopy-Energy Dispersive X-Ray* (SEM-EDX). Hasil analisis XRF menunjukkan bahwa Zn merupakan unsur utama dengan Ag sebagai dopan. Hasil XRD memperlihatkan struktur heksagonal *wurtzite* pada ZnO dan struktur *Face-Centered Cubic* (FCC) pada Ag. SEM-EDX menunjukkan morfologi partikel berukuran nano yang terdistribusi merata. Aktivitas antibakteri diuji dengan metode difusi cakram, dan hasil menunjukkan bahwa zona hambat semakin besar dengan meningkatnya konsentrasi $Zn(NO_3)_2.6H_2O$. Hal ini membuktikan besar nanokomposit ZnO/Ag memiliki aktivitas antibakteri yang efektif terhadap *E.coli*.

1. Introduction

Infections caused by pathogenic bacteria such as Escherichia coli (E.coli) have become a major public health problem worldwide. Altought E.coli is naturally found in the human and animal intestinal microbiota, several strains can act as pathogens, causing diseases such as diarrhea, urinary tract infections, and even sepsis (Kolopita et al., 2022). According to the World Health Organization (WHO), E.coli is among the main causes of diarrhea-related mortality, which contributes to approximately 2.2 million deaths each year, especially among children (WHO, 2015). This situation highlights the urgent need to develop new antibacterial agents that are more effective and environmentally friendly to overcome bacterial infections and the problem of antibiotic resistance.

* Corresponding author.
E-mail address: (a)zeiffamaulita@gmail.com; (b)posman.manurung@fmipa.unila.ac.id

Nanotechnology has emerged as a promising innovation in the search for effective antimicrobial strategies. Zinc oxide (ZnO) has been widely studied because of their broad-spectrum antibacterial activity, including against E.coli (Fatoni et al., 2020). As a nanomaterial, ZnO exhibits unique properties due to its high surface to volume ratio and quantum effects, enabling it to interact effectively with bacterial cells. Additionally, nanocomposite materials formed by combining two nanocstructured components have been proven to enhanced the chemical and biological activity of ZnO, making them more effective for antibacterial applications (Azam et al., 2012).

To improve the antibacterial activity of ZnO, researchers have investigated modifications such as doping with silver (Ag). Ag doping provides a synergistic effect that enhances antibacterial performance by increasing reactive oxygen species (ROS) generation, as well as damaging proteins, DNA, and bacterial metabolic systems (Agarwal et al., 2017). Amrute et al. (2024) reported that Ag-doping decreased the band gap of ZnO from 3.04 eV to 2.81 eV, resulting in higher antibacterial activity. Disk diffusion tests confirmed that Ag doped ZnO produced larger inhibition zones compared to pure ZnO, particularly against E.coli.

The effectiveness of ZnO as an antibacterial agent is also influenced by particle size and morphology. Ragupathi et al. (2011) demonstrated that smaller ZnO nanoparticles showed stronger inhibition against bacteria, with proposed mechanisms including ROS generation and direct penetration into bacterial membranes, leading to cell death. Thus, the synthesis process becomes crucial in determining the performance of nanomaterials. One of the commonly used methods is wet chemical precipitation due to its simplicity, low cost, and ability to produce controlled particle sizes (Chand Gurjar et al., 2023).

The choice of precursor also plays an important role. Zinc nitrate hexahydrate ($Zn(NO_3)_2.6H_2O$) is widely applied in ZnO synthesis because of its high solubility and stable reaction characteristics (Rompis et al., 2020). Variations in $Zn(NO_3)_2.6H_2O$ concentration directly affect crystal growth, morphology, and particle distribution, which ultimately influence antibacterial activity.

Based on these considerations, this study was conducted to synthesize ZnO/Ag nanocomposites with varying concentrations of $Zn(NO_3)_2.6H_2O$ (0.04 M, 0.06 M, 0.08 M, and 0.1 M) using precipitation methods. The objectives are to analyze the composition, structure, and morphology of ZnO/Ag nanocomposites using XRF, XRD, and SEM-EDX, and to evaluate their antibacterial activity against E.coli using the disk diffusion method.

2. Research Methods

2.1 Research Tools and Materials

The tools and materials used in this study include: beaker, furnace, Whatman No.41 filter paper, measuring cylinder, balance, stirring rod, stirrer, spatula, micropipette, hotplate, oven, pH paper, mortar and pestle, petri dish, crucible, furnace, incubator, filter paper, ($Zn(NO_3)_2.6H_2O$) 99% Merck, $AgNO_3$ 99.98% Merck, sodium hydroxide (NaOH) 98% Merck, distilled water (H_2O), ethanol, polyvinyl alcohol (PVA) 93% Sigma Aldrich, E.coli bacterial suspension, XRF PANalytical Epsilon 3, XRD X'Pert Pro PANalytical PW3040/60, and SEM ZEISS EVO MA 10.

2.2 Synthesis of ZnO/Ag Nanocomposites

ZnO/Ag nanocomposites were synthesized using the wet precipitation method with varying concentrations of $Zn(NO_3)_2.6H_2O$: 0.04 M; 0.06 M; 0.08 M; and 0.1 M. The research procedure began with preparing each variation of $Zn(NO_3)_2.6H_2O$ solution concentration (according to molarity calculations) and stirring for 10 minutes until homogeneous. Ethanol and 1 ml of PVA solution were then added to each variation to help stabilize the particle dispersion. The pH of the solution was measured until it reached pH 13 by adding 1 M NaOH solution. When the pH was achieved, 0.1 M $AgNO_3$ solution was added gradually to each $Zn(NO_3)_2.6H_2O$ variation and stirred for 24 hours under closed conditions to prevent contamination and ensure uniform ionic interaction. The mixture was then left at room temperature for 24 hours until a precipitate formed. The precipitate was then filtered using Whatman No.41 paper, dried at 90℃ for 60 minutes, furnace at 100℃ for 1 hour, and heated to 250℃ for 4 hours. The furnace-treated powder is then ground into a fine powder, resulting in ZnO/Ag nanocomposites ready for characterization.

2.3 Antibacterial Test

The antibacterial activity of ZnO/Ag nanocomposites was tested against Escherichia coli using the disk diffusion method. The first procedure involved inoculation E.coli bacteria evenly on the surface of Mueller Hinton Agar (MHA) medium. The discs were then soaked in a solution of ZnO/Ag nanocomposite with varying concentrations of $Zn(NO_3)_2.6H_2O$, and placed on the surface of the MHA medium. As a comparison, discs soaked in gentamicin were used as a positive control, and distilled water as a negative control. All treatments were performed under aseptic conditions to prevent contamination. Petri dishes were incubated at 37℃ for 24 hours. Antibacterial activity was observed through the formation of clear zones around the discs (inhibition zones), whose diameters were measured using a digital caliper in millimeters. The data obtained were then analyzed to determine the effect of variaton in $Zn(NO_3)_2.6H_2O$ concentration on the inhibitory activity of ZnO/Ag nanocomposites againt E.coli.

2.4 Calculation of Particle Size

The particle size of ZnO/Ag nanocomposite crystals can be calculated using XRD data by applying Scherrer's equation shown in **Equation 1**. This equation is used to calculate the crystallite size at a specific Bragg angle.

$$D = \frac{k\lambda}{\beta \cos\theta} \quad (1)$$

where the parameters for **Equation 1** are as follows: D = crystal particle size (nm), K = Scherrer constant (0.9), λ = wavelength of the X-ray used (1.5406 Å), β = Full Width at Half Maximum (FWHM) value (°), and θ = Bragg angle (°)

of the diffraction peak. The calculations were performed on the main diffraction peaks of ZnO and Ag that appear in the XRD pattern. The FWHM values obtained from the diffractogram were then substituted into the Scherrer equation to determine the particle size (Cullity, 1978).

3. Results and Discussions

3.1 XRF Characterization

The results of the XRF characterization analysis of ZnO/Ag nanocomposites with a 1:1 ratio are shown in the **Table 1.**

Table 1. XRF characterization results of ZnO/Ag nanocomposites with variation ZnO (0.1 M).

No.	Element	Element Concentration (%)	Oxidation	Oxidation Concentration (%)
1.	Mg	1.335	MgO	1.602
2.	Si	6.037	SiO_2	4.34
3.	P	1.265	P_2O_5	2.027
4.	K	1.008	K_2O	0.829
5.	Ca	1.105	CaO	1.048
6.	Ti	5.576	TiO_2	6.231
7.	V	0.024	V_2O_5	0.027
8.	Mn	0.016	MnO	0.014
9.	Fe	1.248	Fe_2O_3	1.171
10.	Co	0.016	Co_3O_4	0.014
11.	Zn	61.757	ZnO	58.76
12.	Rb	0.011	Rb_2O	0.007
13.	Sr	0.027	SrO	0.019
14.	Y	0.007	Y_2O_3	0.005
15.	Zr	0.022	ZrO_2	0.018
16.	Nb	0.022	Nb_2O_5	0.019
17.	Ag	10.564	Ag_2O	10.414
18.	Al	9.857	Al_2O_3	13.378
19.	Hf	0.104	HfO_2	0.08
Total		100		100

The analysis results report that Zn was detected in much larger amounts, namely 61.75%, compared to Ag, which was detect at 10.56%. Therefore, ZnO became the matrix in the resulting nanocomposite structure, while Ag was present in small amounts. This difference is attributed to several factors, including the atomic weight difference between the two elements, the differing properties of the precursors used, and the uneven distribution of Ag. Which is deposited in the form of small nanoparticles on the surface of the ZnO matrix. Other elements such as Si (6.04%), Ti (5.6%), Fe (1.3%), and Al (9.8%) were also detected, likely originating from instrument contamination or reagent residues (Asamoah et al., 2020; Zare et al., 2019).

3.2 XRD Characterization

1. Qualitative XRD Analysis. Qualitative XRD analysis was performed to determine the crystalline phases present in the sample. The characterization results for the ZnO/Ag nanocomposite sample with varying ZnO (0.1 M) are presented in the form of a diffractogram shown in **Figure 1**, which illustrates the relationship between relative intensity (a.u.) and diffraction angle ($2\boldsymbol{\theta}$).

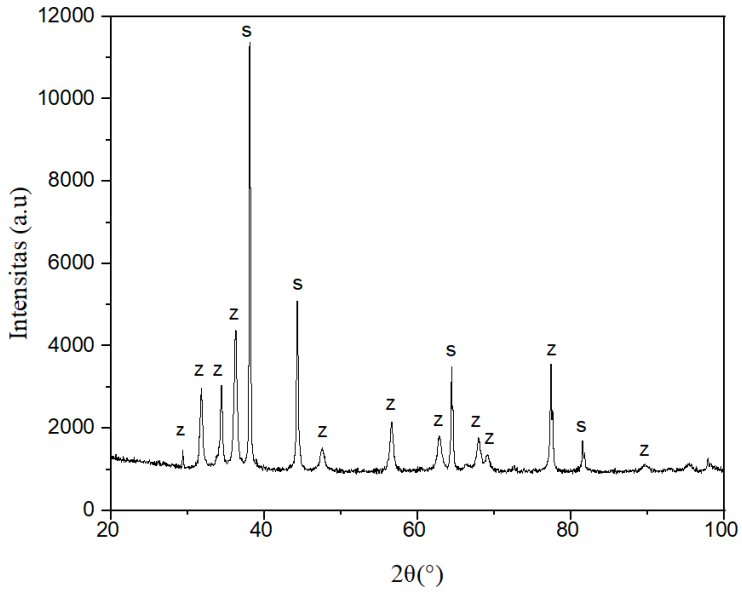

Figure 1. XRD Characterization Results of ZnO/Ag nanocomposites with variations in ZnO (0.1 M). $\lambda = 1.5406$ Å. Legend: z = ZnO and s = Ag.

The X-ray diffraction (XRD) characterization results indicate that the ZnO/Ag nanocomposite with varying ZnO (0.1 M) exhibits the characteristic diffraction pattern of ZnO with a hexagonal wurtzite structure, consistent with JCPDS standard No. 36-1451. The main peaks were detected at 2θ angles of approximately 31.7°, 34.4°, and 36.2°. Additionally, there are additional peaks at 2θ = 38.1° and 44.3°, which are detected as Ag with a face-centered cubic (FCC) structure, consistent with JCPDS standard No. 04-0783. These results confirm that the primary phase formed is ZnO, with Ag present as a dopant that has successfully integrated into the structure (Alharthi et al., 2020).

To identify the phase type, a match was performed between the (2θ) values and the interplanar spacing (d). The results are presented in **Table 2**.

Table 2. Δd Value Difference (Å) in ZnO/Ag Nanocomposite Samples with Variations in ZnO (0.1 M).

No.	Research Data		Standard Data		$\lvert\Delta d$ (Å)$\rvert$	Phase
	2θ (°)	d (Å)	2θ (°)	d (Å)		
1.	31.76	2.815	31.76	2.815	0	ZnO
2.	34.40	2.605	34.46	2.601	0.0044	ZnO
3.	36.27	2.475	36.26	2.475	0.0007	ZnO
4.	38.10	2.360	38.11	2.359	0.0006	Ag
5.	44.25	2.045	44.30	2.043	0.0022	Ag
6.	47.45	1.915	47.57	1.910	0.0045	ZnO
7.	56.62	1.624	56.59	1.625	0.0008	ZnO
8.	62.84	1.478	62.92	1.476	0.0017	ZnO
9.	64.40	1.446	64.44	1.445	0.0008	Ag
10.	67.80	1.381	67.97	1.378	0.0030	ZnO
11.	69.06	1.359	69.08	1.359	0.0003	ZnO
12.	72.46	1.303	72.67	1.300	0.0031	ZnO
13.	77.34	1.233	77.40	1.232	0.0008	Ag
14.	81.48	1.180	81.54	1.180	0.0007	Ag
15.	89.60	1.093	89.66	1.093	0.0006	ZnO

Based on **Table 2**, it shows that the difference in distance between crystal planes between the research data and the standard data is very small, indicating that the crystal structure of the sample has good conformity. This difference is caused by lattice strain and the influence of Ag doping, which causes slight changes in the ZnO lattice parameters. The small Δd values in all data indicate that the crystal structure in the sample is very good and does not experience much distortion (Tran et al., 2013). In addition to determining the phase, the XRD results were also used to determine the size of the crystalline particles formed, as shown in **Table 3**.

Table 3. Peak Height of 2θ Angle and Particle Size of ZnO/Ag Nanocomposite with Variation (0.1 M).

No.	2θ (°)	*Full Width at Half Maximum* (FWHM) (°)	Particle size (nm)
1.	36.27 (ZnO)	0.3247	4.3
2.	38.10 (Ag)	0.1948	7.1

The results in **Table 3** for particle size were obtained from **Equation 1**, which shows that high crystal sizes were obtained in the Ag phase. This was due to differences in crystal growth mechanisms and ion distribution during the synthesis process. For smaller particle sizes, the diffraction peaks had greater sharpness, which was directly related to the degree of crystallinity and homogeneity (Singh et al., 2018).

2. Quantitative XRD Analysis. In addition to qualitative identification, the XRD results were also analyzed quantitatively to determine the percentage of each phase and the cell parameters of each phase formed in the sample. These results were obtained using Rietica version 4.0.5929.62851 software by applying the Rietveld method (Hunter, 1998). Among the many models for ZnO and Ag available in the COD database, the most suitable standard model was found for the ZnO phase (Sawadah et al., 1996) with a hexagonal wurtzite structure and the Ag phase (Suh et al., 1988). After several refinements, this model was the most consistent with the XRD peak pattern of the sample. The results of refining the ZnO/Ag nanocomposite sample with varying ZnO concentrations (0.1 M) are shown in **Figure 2**. In **Figure 2**, the black color represents the XRD data, the red color represents the model, the green color represents the difference in intensity between the two, and the vertical blue line indicates the diffraction peak.

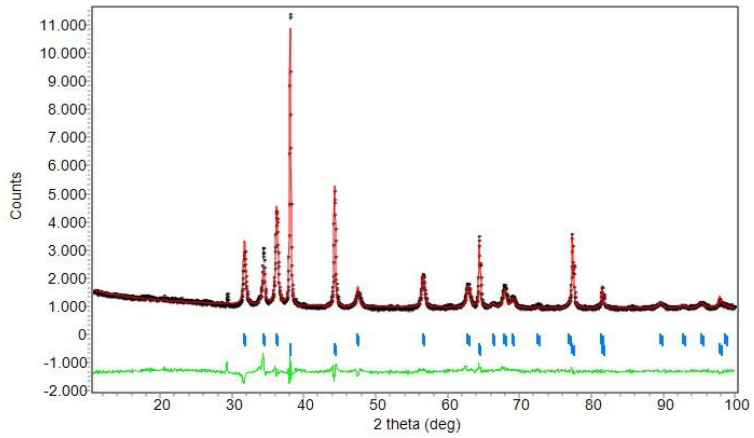

Figure 2. Results of XRD data refinement of ZnO/Ag nanocomposites with varying ZnO (0.1M).

The results of parameter refinement are shown in **Table 4** and the grid parameter cells in **Table 5.**

Table 4. Results of parameter refinement of XRD data for ZnO/Ag nanocomposites with variations of (0.1 M).

Sample	R_{wp}	R_p	R_{exp}	GOF
ZnO/Ag	4.62	3.41	2.89	0.256

Table 5. ZnO/Ag nanocomposite parameter sel with variation (0.1 M).

Phase	Grid Parameters (Å)		
	a	*b*	*c*
Ag	4.0856	4.0856	4.0856
ZnO	3.2499	3.2499	5.2053

The results of the XRD pattern adjustment are shown in **Table 4**, with values of Rp = 3.41, Rwp = 4.62, Rexp = 2.89, and GoF = 0.256, which are still below the tolerance limits (Rp, Rwp < 20% and GoF < 4%), so the refinement results can be considered valid. The lattice parameters obtained are shown in **Table 5**. ZnO has a = b = 3.2499 Å and c = 5.2053 Å, which corresponds to the hexagonal wurtzite structure, while Ag has a = b = c = 4.0856 Å, which corresponds to the cubic structure. The presence of these two phases indicates that the addition of Ag (68%) does not enter the ZnO (32%) lattice but is likely distributed on the surface or between particles (Al-Ariki et al., 2021).

3.3 SEM-EDX Characterization

Morphological characterization and particle size of ZnO/Ag samples using SEM-EDX with 10,000x magnification and a scale of 3 μm on ZnO/Ag samples with varying ZnO (0.1 M). The results of the analysis using SEM-EDX are shown in **Figure 3**.

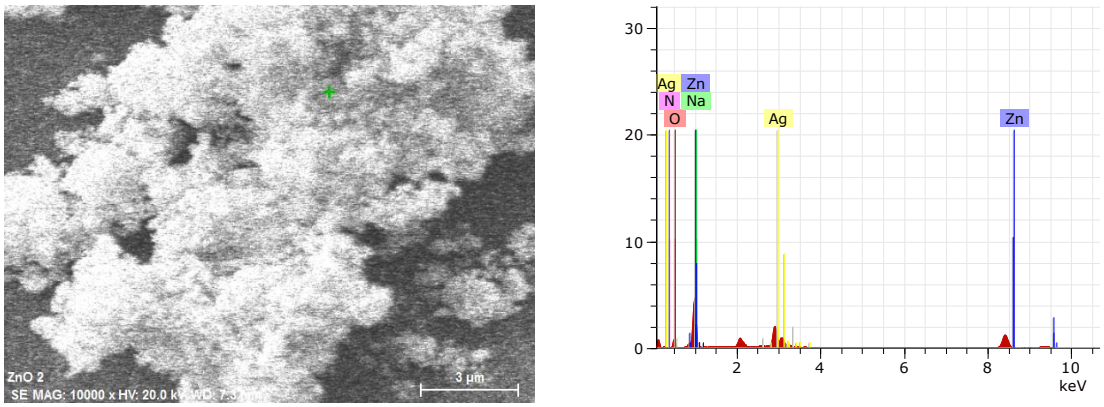

(a) (b)

Figure 3. SEM-EDX Characterization Results (a) Morphological Analysis and (b) Chemical Element Distribution of ZnO/Ag Nanocomposites with varying ZnO (0.1 M).

The morphological results of ZnO/Ag nanocomposites observed by SEM (**Figure 3a**) show that ZnO particles have a relatively uniform shape and a fairly homogeneous size distribution. In addition, Ag particles are evenly distributed among ZnO particles. This indicates that the synthesis process was carried out successfully (Caudra et al., 2022). Based on **Figure 3b**, the X-ray spectrum obtained shows characteristic peaks of the elements Zn and Ag. According to the theory of X-ray emission lines described by Bearden (1967), these peaks are formed due to the transition of electrons from the outer shell to the inner shell of the atom after the inner shell electrons are released due to high-energy electron collisions. For Zn, the main peak appears at an energy of 8.6 keV, which corresponds to the Ka line, while for Ag, the peak is detected at 3 keV, corresponding to the La line. This process occurs when the vacancy in the inner shell is filled by electrons from the outer shell, and the energy difference is emitted in the form of X-ray photons with characteristic energies for each element.

Table 6. Composition Results of ZnO/Ag Nanocomposite with ZnO Variations (0.1 M).

No.	Element	Unnormalized Weight Concentration (wt%)	Normalized Weight Concentration (wt%)	Atomic Concentration (at %)
1.	Oxygen (O)	7.40	39.98	42.47
2.	Zinc (Zn)	2.85	15.43	4.01
3.	Silver (Ag)	7.73	41.80	6.59
4.	Hydrogen (H)	0.51	2.78	46.93
5.	Sodium (Na)	0.00	0.00	0.00
6.	Nitrogen (N)	0.00	0.00	0.00
	Total	18.50	100.00	100.00

The EDX results (**Table 6**) confirm the presence of Zn and Ag elements. The detected Ag content is 41.80% by weight and Zn is 15.43% by weight. The high Ag concentration in this sample is due to the reduction of Ag+ ions to Ag^0 during the synthesis process, which is higher than the formation of ZnO, leading to the accumulation of larger Ag particles (Shrestha et al., 2024). This significant difference can be explained by the difference in atomic mass between the two elements, where Ag has an atomic mass of 107.87 g/mol, which is much larger than Zn with an atomic mass of 65.38 g/mol (Wagh et al., 2023).

3.4. Antibacterial Activity Test

The results of antibacterial activity testing of ZnO/Ag nanocomposites with varying concentrations of ZnO (0.04 M, 0.06 M, 0.08 M, and 0.1 M) against E. coli bacteria using the disk diffusion method are shown in **Figure 4**.

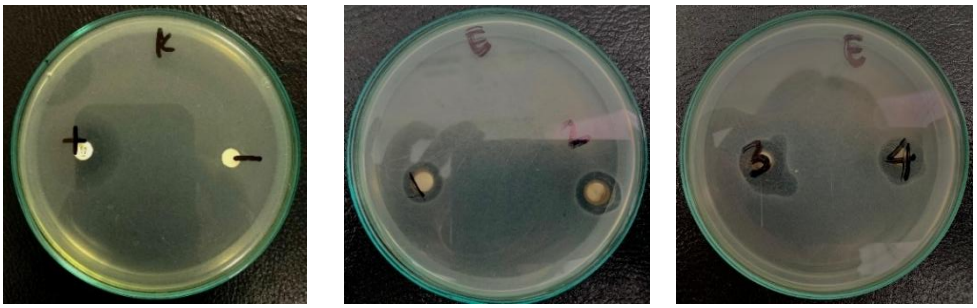

(a) (b) (c)

Figure 4. (a) Results of positive and negative control inhibition zones against E. coli bacteria; (b) and (c) Results of ZnO/Ag nanocomposite inhibition zones against E. coli bacteria. Note: 1 = ZnO/Ag 0.4 M; 2 = ZnO/Ag 0.6 M; 3 = ZnO/Ag 0.8 M; 4 = ZnO/Ag 1 M.

The results of the inhibition zone observations are shown in **Table 7.**

Table 7. Results of Observation of ZnO/Ag Nanocomposite Barrier Zone.

No.	Sample	Inhibition Zone Diameter (mm)
1.	K+	23.72
2.	K-	0
3.	0.04 M	12.46
4.	0.06 M	12.90
5.	0.08 M	15.08
6.	0.1 M	15.21

Based on **Table 7**, the largest inhibition zone diameter was found in the positive control (23.72 mm). In the ZnO/Ag samples, the largest diameter was found at a ZnO concentration of 0.1 M (15.21 mm). This indicates that ZnO-doped ZnO/Ag nanocomposites have an inhibitory effect on the growth of E. coli bacteria, as reported in the study by Raghupathi et al. (2011). In several studies conducted, such as the study by Akbarizadeh et al. (2022), it was shown that the inhibition zone of the ZnO/Ag nanocomposite was larger than that of pure ZnO. This suggests that the antibacterial activity of E. coli can be inhibited by the ZnO/Ag nanocomposite.

Overall, the XRF, XRD, SEM-EDX, and antibacterial tests can be explained through the relationship between material characteristics and performance. The XRF and SEM-EDX results show the dominance of ZnO with Ag as dispersed particles and a morphology that supports the formation of Reactive Oxygen Species (ROS) that damage microbial cell structures. Meanwhile, XRD shows a crystalline structure with nanoparticle-sized phases. All XRF, XRD, and SEM-EDX results directly contribute to the antibacterial test results, where the more optimal the composition, crystalline structure, and morphology, the greater the antibacterial effectiveness.

4. Conclusions

Based on the research results, ZnO/Ag nanocomposites were successfully synthesized by varying the concentration of the $Zn(NO_3)_2{\cdot}6H_2O$ precursor (0.04 M; 0.06 M; 0.08 M; and 0.1 M). XRF characterization results showed that Zn was the dominant element in the material, while Ag was doped in smaller amounts. XRD analysis confirmed that the crystal structure formed was hexagonal wurtzite (ZnO) and Face Centered Cubic (Ag). Meanwhile, SEM-EDX results showed homogeneous particle morphology with uniform element distribution, indicating good material structure quality.

Antibacterial activity testing using the disk diffusion method showed that the higher the concentration of $Zn(NO_3)_2{\cdot}6H_2O$ used, the larger the inhibition zone formed against Escherichia coli bacteria. This proves that ZnO/Ag nanocomposites have good antibacterial efficacy, and this efficacy increases with the increase in ZnO precursor concentration.

Thus, the ZnO/Ag nanocomposite synthesized in this study has the potential to be further developed as a functional material with superior antibacterial properties, making it applicable in the fields of health and the environment.

Acknowledgment

The authors would like to express their gratitude to the Department of Physics, Faculty of Mathematics and Natural Sciences, University of Lampung, for providing the facilities and support necessary to conduct this research. Thanks are extended to the laboratory staff for their assistance during the synthesis and characterization processes. The authors also sincerely appreciate the guidance, encouragement, and valuable input from colleagues and supervisors throughout the completion of this study.

5. Bibliography

Agarwal, H., Venkat Kumar, S., & Rajeshkumar, S. (2017). A review on green synthesis of zinc oxide nanoparticles – An eco-friendly approach. *Resource-Efficient Technologies, 3*(4), 406–413.

Akbarizadeh, M. R., Sarani, M., & Darijani, S. (2022). Study of antibacterial performance of biosynthesized pure and Ag-doped ZnO nanoparticles. *Rendiconti Lincei. Scienze Fisiche e Naturali, 33*(3), 613–621.

Al-Ariki, S., Yahya, N. A. A., Al-A'nsi, S. A., Jumali, M. H. H., Jannah, A. N., & Abd-Shukor, R. (2021). Synthesis and comparative study on the structural and optical properties of ZnO doped with Ni and Ag nanopowders fabricated by sol–gel technique. *Scientific Reports, 11*(1), 1–11.

Alharthi, F. A., Alghamdi, A. A., Al-Zaqri, N., Alanazi, H. S., Alsyahi, A. A., Marghany, A. El, & Ahmad, N. (2020). Facile one-pot green synthesis of Ag–ZnO nanocomposites using potato peel and their Ag concentration dependent photocatalytic properties. *Scientific Reports, 10*(1), 1–14.

Amrute, V., Monika, N., Supin, K. K., Vasundhara, M., & Chanda, A. (2024). Observation of excellent photocatalytic and antibacterial activity of Ag doped ZnO nanoparticles. *RSC Advances, 14*(45), 32786–32801.

Asamoah, R. B., Annan, E., Mensah, B., Nbelayim, P., Apalangya, V., Onwona-Agyeman, B., & Yaya, A. (2020). A comparative study of antibacterial activity of CuO/Ag and ZnO/Ag nanocomposites. *Advances in Materials Science and Engineering, 2020*, 1–18.

Azam, A., Ahmed, A. S., Oves, M., Khan, M. S., Habib, S. S., & Memic, A. (2012). Antimicrobial activity of metal oxide nanoparticles against gram-positive and gram-negative bacteria: A comparative study. *International Journal of Nanomedicine, 7*, 6003–6009.

Bearden, J. A. (1967). X-ray wavelengths. *Reviews of Modern Physics, 39*(1), 78–124.

Chand Gurjar, K., Agrawal, A., Kumar, S., Sharma, R., Pandey, K., Pandey, H., & Awasthi, A. (2023). Antimicrobial efficacy of Ag-doped ZnO nanocomposite against *Bacillus subtilis*. *Materials Today: Proceedings, 95*, 61–66.

Cuadra, J. G., Scalschi, L., Vicedo, B., Guc, M., Izquierdo-Roca, V., Porcar, S., Fraga, D., & Carda, J. B. (2022). ZnO/Ag nanocomposites with enhanced antimicrobial activity. *Applied Sciences, 12*(10), 1–13.

Cullity, B. D. (1978). *Elements of X-ray diffraction* (2nd ed.). Addison-Wesley.

Fatoni, A., Hilma, H., Rasyad, A. A., Novriyanti, S., & Hidayati, N. (2020). Biosintesis ZnO nanopartikel dari ekstrak air daun jambu biji (*Psidium guajava* L.) dan ion Zn2+ serta interaksinya dengan kitosan sebagai antibakteri *Escherichia coli*. *Jurnal Sains Farmasi & Klinis, 7*(2), 151–158.

Hunter, B. A. (1998). Rietica – A visual Rietveld program. *Commission on Powder Diffraction Newsletter, 20*, International Union of Crystallography.

Kolopita, P. S., Hariyadi, H., Sambou, C. N., & Tulandi, S. S. (2022). Uji aktivitas antibakteri kulit batang alpukat (*Persea americana* Mill.) terhadap bakteri *Staphylococcus aureus* dan *Escherichia coli*. *Majalah INFO Sains, 3*(1), 19–26.

Raghupathi, K. R., Koodali, R. T., & Manna, A. C. (2011). Size-dependent bacterial growth inhibition and mechanism of antibacterial activity of zinc oxide nanoparticles. *Langmuir, 27*(7), 4020–4028.

Rompis, J., Aritonang, H., & Pontoh, J. (2020). Sintesis nanokomposit ZnO–MgO dan analisis efektivitas sebagai antibakteri. *Chemistry Progress, 13*(1), 56–62.

Sawadah, H., Wang, R., & Sleght, A. W. (1996). An electron density residual study of zinc oxide. *Journal of Solid State Chemistry, 122*, 148–150.

Shrestha, D. K., Magar, A. B., Bhusal, M., Baraili, R., Pathak, I., Joshi, P. R., Parajuli, N., & Sharma, K. R. (2024). Synthesis of silver and zinc oxide nanoparticles using *Polystichum lentum* extract for potential antibacterial, antioxidant, and anticancer activities. *Journal of Chemistry, 2024*, 1–15.

Singh, J., Dutta, T., Kim, K. H., Rawat, M., Samddar, P., & Kumar, P. (2018). Green synthesis of metals and their oxide nanoparticles: Applications for environmental remediation. *Journal of Nanobiotechnology, 16*(1), 1–24.

Suh, I. K., Ohta, H., & Waseda, Y. (1988). High-temperature thermal expansion of six metallic elements measured by dilatation method and X-ray diffraction. *Journal of Materials Science, 23*, 757–760.

Tran, Q. H., Nguyen, V. Q., & Le, A. T. (2013). Silver nanoparticles: Synthesis, properties, toxicology, applications and perspectives. *Advances in Natural Sciences: Nanoscience and Nanotechnology, 4*(3), 033001.

Wagh, S. S., Kadam, V. S., Jagtap, C. V., Salunkhe, D. B., Patil, R. S., Pathan, H. M., & Patole, S. P. (2023). Comparative studies on synthesis, characterization and photocatalytic activity of Ag doped ZnO nanoparticles. *ACS Omega, 8*(8), 7779–7790.

World Health Organization. (2015). *Global action plan on antimicrobial resistance*. World Health Organization.

Zare, M., Namratha, K., Alghamdi, S., Mohammad, Y. H. E., Hezam, A., Zare, M., Drmosh, Q. A., Byrappa, K., Chandrashekar, B. N., Ramakrishna, S., & Zhang, X. (2019). Novel green biomimetic approach for synthesis of ZnO–Ag nanocomposite: Antimicrobial activity against food-borne pathogen, biocompatibility and solar photocatalysis. *Scientific Reports, 9*(1), 1–15.